Equinatoxin II Permeabilizing Activity Depends on the Presence of Sphingomyelin and Lipid Phase Coexistence

Peter Schön,* Ana J. García-Sáez,* Petra Malovrh,† Kirsten Bacia,* Gregor Anderluh,† and Petra Schwille*
*Biophysics Group, BIOTEC, TU Dresden, Dresden, Germany; and †Department of Biology, Biotechnical Faculty, University of Ljubljana, Slovenia

ABSTRACT Equinatoxin II is a pore-forming protein of the actinoporin family. After membrane binding, it inserts its N-terminal α-helix and forms a protein/lipid pore. Equinatoxin II activity depends on the presence of sphingomyelin in the target membrane; however, the role of this specificity is unknown. On the other hand, sphingomyelin is considered an essential ingredient of lipid rafts and promotes liquid-ordered/liquid-disordered phase separation in model membranes that mimic raft composition. Here, we used giant unilamellar vesicles to simultaneously investigate the effect of sphingomyelin and phase separation on the membrane binding and permeabilizing activity of Equinatoxin II. Our results show that Equinatoxin II binds preferentially to the liquid-ordered phase over the liquid-disordered one and that it tends to concentrate at domain interfaces. In addition, sphingomyelin strongly enhances membrane binding of the toxin but is not sufficient for membrane permeabilization. Under the same experimental conditions, Equinatoxin II formed pores in giant unilamellar vesicles containing sphingomyelin only when liquid-ordered and -disordered phases coexisted. Our observations demonstrate the importance of phase boundaries for Equinatoxin II activity and suggest a double role of sphingomyelin as a specific receptor for the toxin and as a promoter of the membrane organization necessary for Equinatoxin II action.

INTRODUCTION

Pore-forming toxins (PFTs) are a group of toxic molecules that exert their action by increasing the permeability of their target membranes. As a consequence, ion gradients are disrupted, which provokes osmotic swelling and cell death (1). An interesting trait common to all PFTs is that they present two stable structures: they are synthesized as water-soluble monomers, and they insert into cell membranes to exert their action (2). Then, PFTs follow a variety of mechanisms to induce the formation of membrane pores (3). Some of them, like bacterial cytolysins and the staphylococcal α-toxin, form β-barrel channels (4,5). Others induce pores by insertion of α-helices: they organize into pure protein α-helix bundles, such as the antimicrobial peptide alamethicin, or form mixed lipid/protein structures known as toroidal pores (as in the case of actinoporins, colicins, and magainin or melittin) (6). Toroidal pores are unstable and have not yet been visualized. As a consequence, little structural information is available (7).

Equinatoxin II (EqtII) belongs to the family of actinoporins, eukaryotic PFTs exclusively found in sea anemones, whose activity depends on the presence of sphingomyelin (SM) in the target membrane (8). It efficiently lyses several cell types and shows permeabilizing activity in model membranes. The structure of the water-soluble form of EqtII has been determined (9,10). It contains 179 amino acids (19.8 kDa) that arrange into a hydrophobic β-sandwich core surrounded by two α-helices on both sides. The first 30 N-terminal residues contain an α-helix that undergoes conformational changes during membrane insertion and pore formation (11). The flexibility of this α-helix is necessary for EqtII activity (12).

Some aspects of the mechanism of action of EqtII at the molecular level have been unveiled during the past few years. It includes an initial step of membrane binding, in which a cluster of exposed aromatic residues is involved (12–14). Then, the N-terminal helix dissociates from the β-sandwich core, inserts into the lipid-water interface, and adopts an orientation parallel to the membrane plane (3,11). Subsequently, EqtII monomers oligomerize and the N-terminal helix reorients and crosses the bilayer to form the pore (11,15). Several studies suggest that the EqtII pore is formed by 3–4 monomers that arrange into a toroidal structure lined by N-terminal α-helices and lipids (16,17).

The role of SM in target membrane specificity is unknown. It is essential for irreversible binding of EqtII and pore formation, but it is not sufficient to provoke the dissociation of the N-terminal helix from the β-sandwich in the presence of phosphatidylcholine micelles and bicelles (18). On the other hand, SM is a substantial ingredient of lipid rafts, which are supposedly associated to the coexistence of liquid-disordered (L_d) and SM-enriched liquid-ordered (L_o) lipid phases (19). In this context, phase coexistence in SM-containing membranes has been suggested to favor membrane insertion of EqtII into the lipid packing defects at the interface (20).

During the past few years, giant unilamellar vesicles (GUVs) have been proven to be valuable models for the study

Submitted January 21, 2008, and accepted for publication March 18, 2008.

Address reprint requests to Petra Schwille, Tatzberg 47-51, 1307 Dresden, Germany. Tel.: 49-351-4634-0328; E-mail: petra.schwille@biotec.tu-dresden.de.

Kirsten Bacia's present address is Dept. of Molecular and Cell Biology, University of California, Berkeley, CA.

Editor: Thomas J. McIntosh.

0006-3495/08/07/691/08 $2.00

doi: 10.1529/biophysj.108.129981

of processes at lipid membranes. With diameters varying from a few to a hundred microns, GUVs have sizes comparable to eukaryotic cells and are well distinguished by optical microscopy. In addition to studies of membrane elasticity and shape change (21,22), GUVs have been especially useful for the investigation of phase-separating membranes and lipid domains (23–25). In GUVs with raft-like composition, macroscopic domains corresponding to L_o, enriched in SM, and L_d phases can be clearly distinguished thanks to heterogeneous partitioning of fluorescent markers (25,26). GUVs have also been used to study membrane permeabilization (27,28) and the effect of EqtII pores on the transport of sucrose and glucose molecules (29). The main advantage of using GUVs versus the traditional methods based in small and large unilamellar vesicles (LUVs) is that optical measurements can be performed at the single-vesicle and even single-molecule level while tracking membrane integrity. This provides novel information about the mechanism of pore formation.

In this work, we used GUVs to simultaneously investigate the role of SM and lipid phase coexistence in the membrane binding and permeabilizing activity of EqtII. Our results show that EqtII binds preferentially to the SM-enriched L_o phase over the L_d phase. Interestingly, it concentrates at the domain interface. Although the presence of SM strongly promoted membrane binding, SM in a single-phase membrane was not sufficient for membrane permeabilization. At the same protein concentration, EqtII was able to permeabilize SM-containing GUVs only when L_d and L_o phases coexisted. Our observations demonstrate the importance of the phase interface for EqtII activity and suggest that SM has a pivotal role in acting as a specific receptor for EqtII while promoting the membrane organization necessary for EqtII action.

MATERIALS AND METHODS

Chemicals

1,2-Dioleoyl-*sn*-glycero-3-phosphocholine (dioleoyl-phosphatidylcholine; DOPC), 1,2-dipalmitoyl-*sn*-glycero-3-phosphocholine (DPPC), *N*-stearoyl-D-erythrosphingosylphosphorylcholine (stearoyl SM), and cholesterol were purchased from Avanti Polar Lipids (Alabaster, AL). 1,1′-Dioctadecyl-3,3,3′,3′-tetramethylindodicarbocyanine perchlorate (DiD) and 1,1′-dioctadecyl-3,3,3′,3′-tetramethylindocarbocyanine perchlorate (DiI) were from Invitrogen (Carlsbad, CA).

Protein purification and labeling

Two single-cysteine mutants of EqtII, EqtII-V22C, and EqtII-L26C were produced as in Malovrh et al. (11). The two purified mutants EquII-V22C and EquIIL-26C were labeled with Alexa Fluor 488 C_5 maleimide (Invitrogen) according to the manufacturer's instructions. The separation of the labeled protein from the free dye was achieved by a 10DG gel filtration column from Bio-Rad (Hercules, CA), and the labeling was checked by spectroscopy measurements done with a Specord S 100 from Analytik Jena (Jena, Germany).

Preparation of giant unilamellar vesicles

GUVs were prepared by electroformation (30). With this approach, truly unilamellar vesicles are produced with sizes varying from 10 μm to 100 μm. The electroformation chamber consists of two glass slides coated with optically transparent and electrically conductive indium tin oxide that are held apart by a Teflon or rubber spacer. A total of 3 μl of the corresponding lipid mixture (10 mg/ml) together with 0.1% DiD or DiI (31) in chloroform/methanol 2:1 were deposited on the preheated indium tin oxide glasses, and the solvent was evaporated at 65°C. After adding a 300 mM sucrose solution to the chamber, a voltage of 1.4 V at 10 Hz was applied overnight. The electroformed vesicles were then carefully pipetted out of the electroformation chamber and sedimented in 800 μl phosphate buffer saline (PBS; 137 mM NaC, 10 mM phosphate, 2.7 mM KCl, pH 7.4). After a few minutes, either 150 μl were pipetted out from the bottom of the tube and distributed into the four compartments of the observation chamber (Invitrogen) or 200 μl from several GUV-containing tubes were combined and gently mixed, and then an eight-well observation chamber was filled with 100 μl per well. All preparation steps were done at 65°C to avoid lipid demixing. During cool-down to room temperature in the observation chambers, phase separation into L_o and L_d phases occurs, with DiD and DiI almost exclusively distributing into the L_d phase.

Confocal microscopy

Images were obtained at room temperature by confocal fluorescence microscopy, performed on a commercial ConfoCor3 from Zeiss (Jena, Germany) with a laser scanning microscopy module. The excitation light of an Ar ion laser at 488 nm and of a helium-neon laser at 633 nm was reflected by a dichroic mirror (HFT 488/633) and focused through a Zeiss C-Apochromat 40×, NA = 1.2 water immersion objective onto the sample. The fluorescence emission was recollected by the same objective and split by another dichroic mirror (NFT 545) into two channels. Detection of the fluorescence emission, after passing a 505–530 nm band-pass filter in the first channel and a 650 nm long-pass filter in the second channel, was obtained with two avalanche photodiodes.

Measurements of membrane binding and permeabilization

Protein binding distributions were calculated by sampling over several vesicle preparations. We quantified the fluorescence intensities of EqtII-Al488 in the L_o and the L_d phases within a single vesicle and calculated the intensity ratio I_F^{Lo}/I_F^{Ld} half an hour after the addition of ~10 μg/ml (final concentration) of one of the labeled EqtII mutants.

Pore activity measurements were done by adding a PBS solution containing Alexa Fluor 488 (molecular mass 720 Da) as a marker as well as the unlabeled EqtII to the vesicles and gently mixing the sample to achieve a largely homogeneous distribution of vesicles, marker, and protein. After 45 min the number of GUVs into which the marker had penetrated was counted versus the total number of vesicles in several regions of the sample. Up to 600 vesicles were evaluated per data point.

The degree of filling was determined by taking a sample image every 30 s and comparing the intensity of the fluorescence marker within a vesicle with the intensity just outside the GUV.

RESULTS

EqtII prefers the L_o over the L_d phase and concentrates at the domain interface

EqtII binding and insertion into lipid membranes is affected by the presence of SM (17), which is related to cellular lipid rafts (19). Model membranes that contain SM, DOPC, and cholesterol in a raft-like composition show the coexistence of L_d and L_o phases (26,31,33,34). The L_o phase is enriched in SM and is characterized by conformational order in the lipid

acyl chains, whereas their lateral and rotational lipid mobility is more similar to the L_d phase than to the gel phase (19).

To investigate the effect of membrane phase and composition on the binding affinity of EqtII, we performed binding experiments in GUVs with different lipid mixtures. As explained in Materials and Methods, two EqtII mutants were labeled to homogeneity and used for experiments. The mutations used were from the N-terminal region, which is not close to the region of the molecule that interacts with the lipid membrane (12,13,18). In our experiments, the two mutants showed exactly the same behavior, both in binding and permeabilization. When the mutant is not specified, the general name EqtII-Al488 is used to denote results obtained for both labeled mutants.

We added EqtII-Al488 to GUVs that contained SM and to GUVs that did not contain SM, with only L_d or L_o phase, or L_d-L_o phase coexistence. The membranes were labeled with DiD or DiI, which partition preferentially to the L_d phase (25). After 30 min incubation, we checked for membrane binding by confocal microscopy. As observed in Fig. 1, EqtII-Al488 binds preferentially to vesicles containing SM. In Fig. 1, *E–H*, a control without SM (lipid composition DOPC/cholesterol (1:1)) shows no membrane binding of the toxin under these conditions. When EqtII-V22C-Al488 was added to a mixture of SM-containing GUVs with only the L_o (SM/cholesterol, 1:1) or L_d (SM/DOPC, 1:1) phase (25), the toxin bound preferentially to the vesicles in the L_o phase (see Fig. 1, *A–D*). Fig. 1, *I–N*, depicts the binding of Alexa-488-labeled mutants of EqtII to GUVs containing SM and exhibiting L_d-L_o phase coexistence (DOPC/SM/cholesterol, 1:1:1). The three-dimensional projections of representative GUVs show that the toxin binds preferentially to the SM-enriched L_o phase over the L_d phase. Interestingly, intense dots of EqtII-L26C-Al488 localize at some of the phase boundaries, indicating the tendency of the protein to concentrate at the interface.

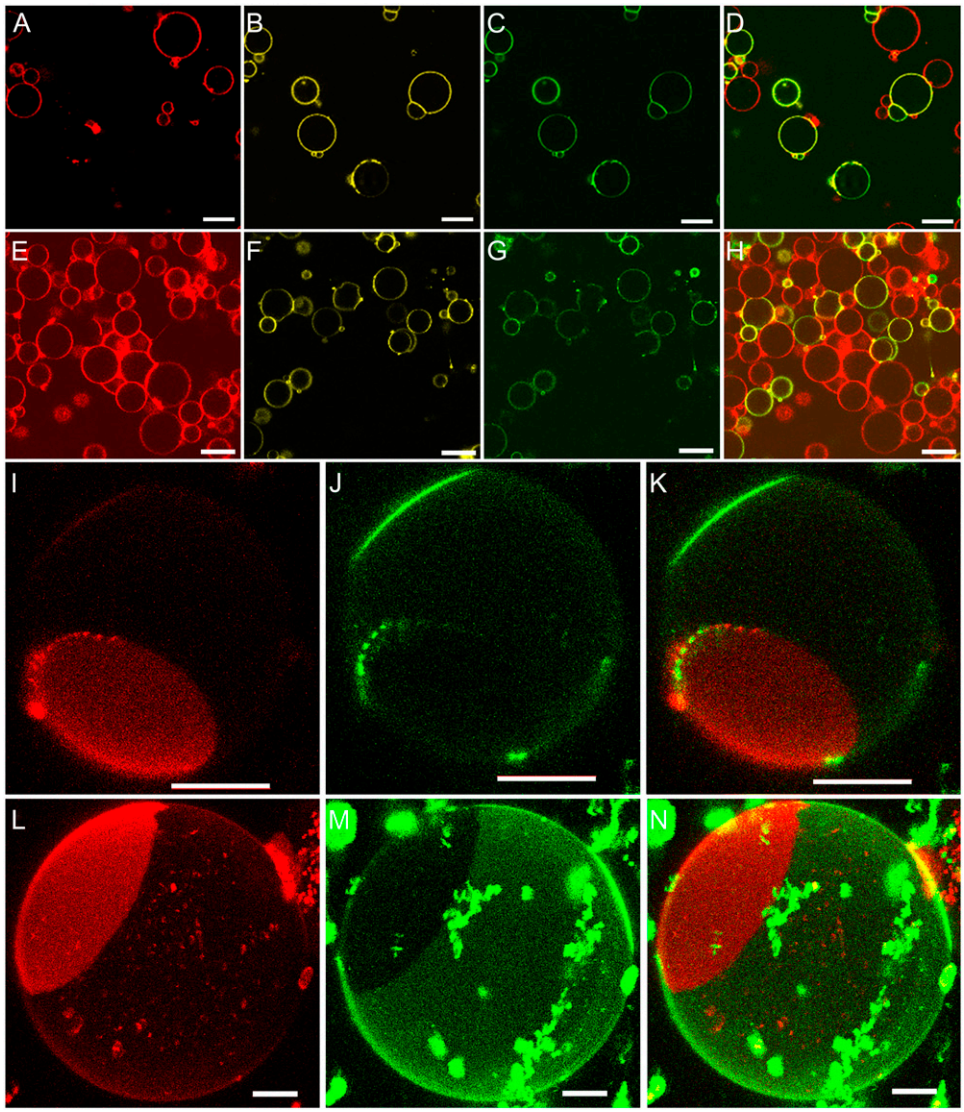

FIGURE 1 Effect of lipid composition on membrane binding of EqtII-Al488. EqtII-Al488 was added to GUVs containing DiD or DiI, which are lipophilic dyes that label specifically the L_d phase. Vesicles labeled with DiD are depicted in red, DiI is depicted in yellow, and the fluorescent mutants of EqtII are depicted in green. (*Top row*) Mixture of GUVs composed of DOPC/SM (1:1) 0.1% DiD (*A*) and SM/Chol (1:1) 0.1% DiI (*B*) 30 min after addition of EqtII-V22C-Al488 (*C*). Merge shown in *D*. (*Second row*) Mixture of GUVs composed of DOPC/Chol (1:1) 0.1% DiD (*E*) and SM/Chol (1:1) 0.1% DiI (*F*) after addition of EqtII-V22C-Al488 (*G*). Merge shown in *H*. Scale bars, 20 μm. (*Third* and *fourth rows*) DOPC/SM/Chol (1:1:1) 0.1% DiD (*I* and *L*), EqtII-V22C-Al488 (*J*), and EqtII-L26C-Al488 (*M*), merge in *K* and *N*. For clarity, the L_o / L_d intensity ratios of EqtII mutants in the third and fourth rows are 1.5 and 4, respectively. Scale bar, 10 μm.

Assuming that the fluorescence intensity in GUVs is proportional to EqtII-Al488 concentration, we quantified the phase binding preference of EqtII-Al488 by calculating the partitioning of the protein between both L_o and L_d phases in a large number of different vesicles. The results obtained are represented in Fig. 2 and include data from both mutants. The spread of the data is indicative of the heterogeneity of the system. EqtII-Al488 bound more extensively to the L_o phase in the majority of the vesicles (69%), ranging from a 1.5-fold to a 10-fold preference for this phase. A minor number of vesicles exhibited homogeneous distribution or higher concentration in the L_d phase.

EqtII pore-forming activity depends on the presence of phase separation

To determine whether the differences observed in binding affinity have an effect on the pore-forming activity of EqtII, we carried out experiments of membrane permeabilization in GUVs. GUVs of the desired lipid compositions were prepared, and Alexa-488 together with unlabeled EqtII was added to the external solution. Vesicle permeabilization caused an increase in fluorescence intensity inside the GUVs, indicative of filling with Alexa-488. Such a system allows simultaneous verification of vesicle integrity and L_d-L_o phase coexistence while measuring pore activity.

Fig. 3 shows the vesicles immediately after the addition of Alexa-488 and EqtII to the external medium (Fig. 3, *A–D*) and after 45 min of incubation at room temperature (Fig. 3, *E–H*). In all cases vesicles retained their integrity upon toxin treatment. The GUVs in Fig. 3, *A* and *E*, were made of DOPC/cholesterol (1:1) and were not permeabilized after incubation with EqtII. Under similar conditions, EqtII showed pore-forming activity in vesicles composed of DOPC/SM/cholesterol (1:1:1), which exhibit L_d-L_o phase separation (Fig. 3, *C* and *G*). However, GUVs containing SM but no phase coexistence (SM/cholesterol, 1:1) were not permeabilized by EqtII (Fig. 3, *B* and *F*), despite toxin binding to the membrane (as shown in Fig. 1, *E–H*). As a control, bovine serum albumin (BSA) was added to GUVs made of DOPC/SM/cholesterol (1:1:1), and only rare vesicle permeabilization was observed (Fig. 1, *D* and *H*).

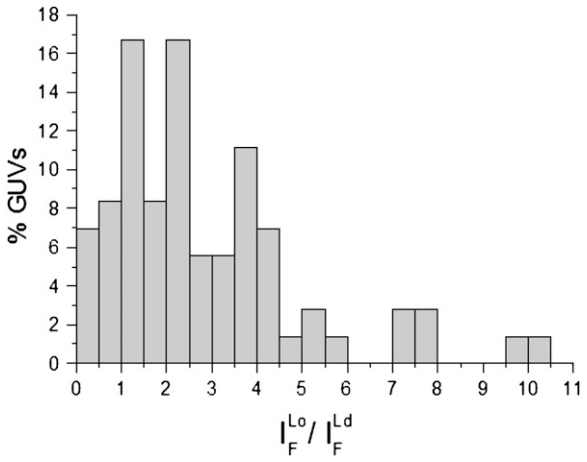

FIGURE 2 Partition of EqtII-Al488 between the L_d and L_o phases. Fluorescence intensity was measured 30 min after adding ~10 μg/mL of any of the EqtII-Al488 mutants to GUVs of lipid composition DOPC/SM/cholesterol (1:1:1), 0.1% DiD. The ratio of EqtII-Al488 in the L_d and L_o phases was calculated for 72 vesicles and plotted as a normalized histogram. Bin size, 0.5.

These observations indicate that phase separation has a strong effect on promoting EqtII pore-forming activity. To check this possibility, we measured EqtII permeabilizing activity in GUVs composed of DOPC/DPPC/cholesterol (1:1:1), which do not contain SM but do exhibit a phase coexistence. As summarized in Table 1, under the same conditions, EqtII was able to permeabilize 67% of vesicles, in comparison with 98% activity in DOPC/SM/cholesterol (1:1:1). Interestingly, the addition of SM to only 5% (DOPC/DPPC/cholesterol/SM, 1:1:1:0.16) recuperated the activity of EqtII to 96%. Our results indicate that the coexistence of L_d and L_o phases is enough to enhance the pore-forming activity of EqtII and that the presence of SM has a synergistic effect by increasing EqtII binding to the membrane.

Permeabilization of GUVs is a stochastic and fast event

Bulk experiments of vesicle permeabilization show cooperative behavior in the concentration-dependent activity of many PFTs, including EqtII (17,35–38). In contrast to traditional assays of content release from LUVs (which provide information about the average permeabilization from all the LUVs in the suspension), permeabilization experiments in GUVs provide information about events at the single vesicle level (they analyze the fraction of the permeabilized vesicles among all the examined ones). To check if the information obtained from GUVs is comparable to content release experiments in LUVs, we measured the pore activity of EqtII at several protein concentrations. Fig. 4 shows the percentage of vesicles permeabilized as a function of the toxin concentration. The activity curve obtained is similar to the results obtained in bulk experiments (17). Under our experimental conditions, 50% of vesicles were permeabilized at ~4.3 μg/mL of EqtII.

In addition to average activity, experiments of GUV permeabilization allow us to investigate the filling kinetics of single vesicles. Fig. 5 *A* shows the grade of vesicle filling as a function of time for several individual vesicles. In general, membrane permeabilization started at ~20 min after mixing the GUVs with EqtII. After this lag time, the increase of fluorescence intensity inside the vesicles started stochastically, and complete filling was rapidly achieved within times varying from ~1–5 min.

From these data, we can calculate the volume flux J_V through the membrane. Assuming a constant fluorophore

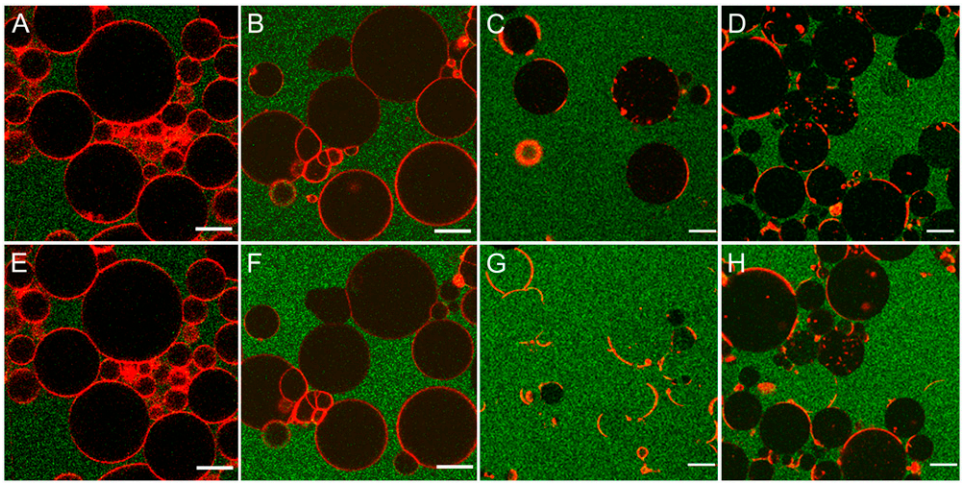

FIGURE 3 Effect of membrane phase and composition on the permeabilizing activity of EqtII. (*A–C*) The samples immediately after adding 30 μg/mL of EqtII-L26C (first column) or EqtII-V22C (second and third columns), or the same amount of BSA in the forth column. (*E–H*) The same samples as *A–D* after 45 min incubation at room temperature. Lipid composition of GUVs: (*A* and *E*) DOPC/cholesterol (1:1) 0.1% DiI; (*B* and *F*) SM/cholesterol (1:1) 0.1% DiD; (*C*, *D*, *G*, and *H*) DOPC/SM/cholesterol (1:1:1) 0.1% DiD. DiD and DiI specifically label the L_d phase and for clarity are depicted in red. The surrounding solution was colored with Alexa-488 (*green*) at 300 nM. The scale bars correspond to 20 μm.

concentration c_{ext}, set to 1 for simplicity, the fluorophore concentration $c(t)$ inside a GUV will change during the time interval dt in this manner:

$$c(t+dt) = c(t) + \frac{dN_{ext\to i} - dN_{i\to ext}}{V_i}, \quad (1)$$

where $dN_{ext\to i}$ and $dN_{i\to ext}$ are the fluorophores that cross the membrane from the outside to the inside and vice versa, respectively, and V_i is the vesicle volume, also assumed to be constant. With $c = N/V$. this leads to

$$c(t+dt) = c(t) + \frac{1-c(t)}{V_i}dV = c(t) + \frac{1-c(t)}{V_i}J_V A dt \quad (2)$$

with A as the vesicle surface. Since the GUVs can be regarded as spheres, $A = 4\pi R^2$, and $V = 4\pi/3R^3$, the above expression can be written as the differential equation:

$$c'(t) = \frac{3J_V}{R}(1 - c(t)). \quad (3)$$

The starting condition $c(0) = c_0 = 0$ yields the solution

$$c(t) = 1 - e^{-\frac{3J_V}{R}t}. \quad (4)$$

Expressed as in Eq. 5, the slope of the curve directly shows the volume flux J_V:

$$-\frac{R}{3}\ln(1 - c(t)) = J_V t. \quad (5)$$

TABLE 1 Effect of SM and phase separation on the permeabilizing activity of EqtII-AI488

Lipid composition	Percent of filled GUVs
DOPC/SM/cholesterol (1:1:1)	98 ± 1
DOPC/DPPC/cholesterol (1:1:1)	67 ± 4
DOPC/DPPC/cholesterol/SM (1:1:1:0.16)	96 ± 2

In all cases, a total number of at least 500 vesicles was counted. The error bars correspond to a counting error of 10%.

Table 2 shows the volume flux J_V in the individual vesicles, calculated from the slopes in Fig. 5 *B* according to Eq. 5. The spread values obtained show the heterogeneity of the filling process, which gives an average filling flux of 8 ± 5 μm/min.

DISCUSSION

Permeabilization of single vesicles

We used a similar approach to Yamazaki and co-workers for membrane permeabilization studies in single GUVs (28,39). Our results show that membrane permeabilization by EqtII in single vesicles was comparable to bulk experiments when averaged. But in addition, they allowed us to confirm vesicle integrity during permeabilization and to simultaneously measure the filling kinetics at the single vesicle level. We observed that after addition of the toxin, a lag time of ~20 min was necessary for pore formation. A similar behavior

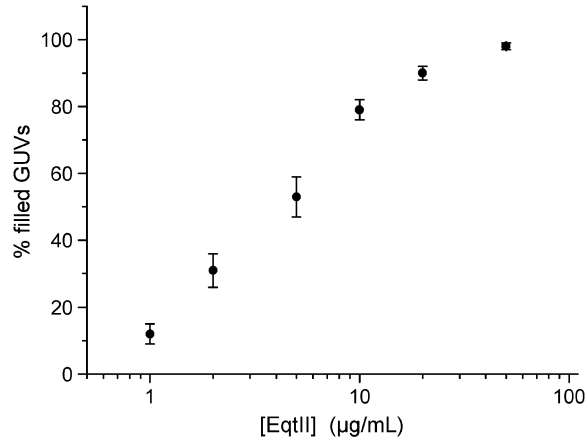

FIGURE 4 Permeabilization activity of EqtII in GUVs as a function of toxin concentration. Pore activity was calculated as the percentage of filled vesicles 45 min after addition of EqtII-V22C. Between 200 and 300 vesicles were considered for each data point. The error bars correspond to a counting error of 10%. Vesicles are composed of DOPC/SM/cholesterol (1:1:1) 0.1% DiD.

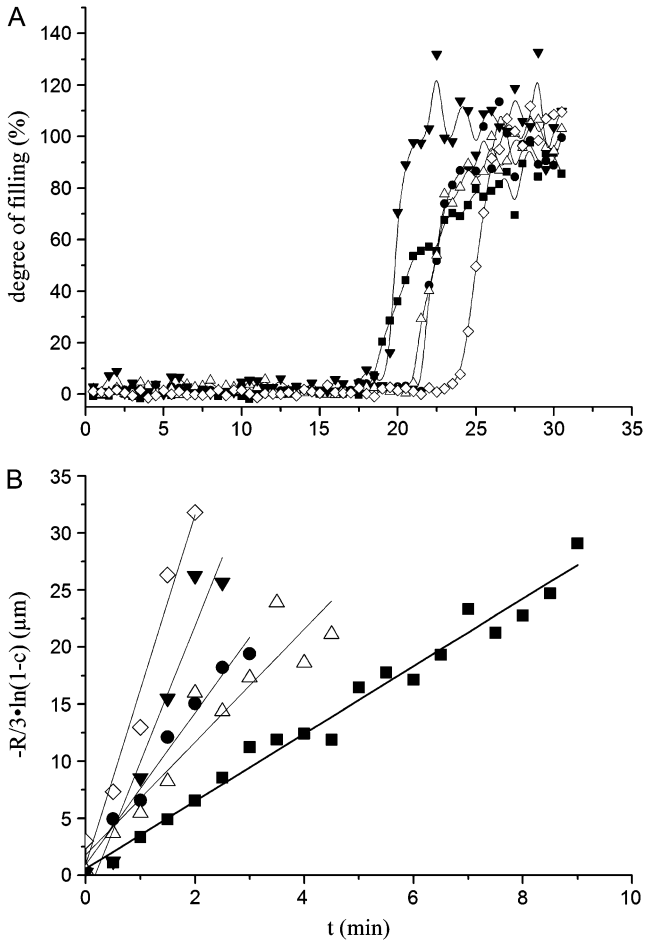

FIGURE 5 Kinetics of a single vesicle filling. (*A*) Filling grade of several individual vesicles as a function of time. Experimental conditions correspond to 10 μg/mL of EqtII-L26C added to sample GUVs composed of DOPC/SM/cholesterol (1:1:1) 0.1% DiD. (*B*) Dye flux into the same individual vesicles, expressed according to Eq. 5.

was obtained in bulk experiments of vesicle permeabilization and hemolysis (17). Since binding to lipid membranes occurs in seconds (12), processes like oligomerization, conformational changes, and insertion of the N-terminus α-helix probably contribute to the lag time. This is also in agreement with the two-state model of pore formation by Huang and colleagues (40). According to this model, toxin binding to the outer leaflet would introduce additional area, so that a stress in the membrane, or membrane tension, would be created. After enough toxin molecules have bound, the membrane tension generated would destabilize the bilayer and provoke pore opening. Though, to our knowledge, no membrane-thinning effect has been measured for EqtII to date, insertion of the N-terminal α-helix of EqtII, which is related to pore formation (3,15), has been shown to increase the lateral pressure in monolayers (12).

The variations in the lag time for pore formation measured in the individual vesicles are probably related to the heterogeneities in the system and the stochastic nature of pore

TABLE 2 Dye flux *J* into single GUVs permeabilized by EqtII-AI488

Vesicle	Radius (μm)	*J* (μm/min)
1	44	3.0
2	27	6.6
3	32	4.9
4	21	12.0
5	32	15.3

J values were calculated from the slopes in Fig. 5 *B* according to Eq. 5.

opening (28). Once pore opening took place, vesicle filling was fast and complete within a few minutes. This is in the same time range observed for other molecules, like magainin or epigallocatechin gallate (28,39). We derived an equation to calculate the rate of vesicle filling. The differences observed in the estimated filling fluxes may arise from a different number of pores per vesicle, from pores with different sizes, and/or from a different Laplace pressure in the individual vesicles (41).

Role of SM in EqtII activity

The presence of SM enhances the binding of EqtII to the membrane (20). Although the molecular basis for this lipid specificity is unknown, SM is necessary for the irreversible binding of the toxin to the membrane, which is followed by insertion and pore formation (42). However, as shown by NMR studies, SM is not sufficient to trigger the conformational change that inserts the N-terminal α-helix responsible for pore opening, at least in micelle and bicelle model membrane systems (18). Though EqtII also interacts with lipid membranes in the absence of SM, our observations in GUVs clearly evidence a preference for the binding to SM-containing vesicles and highlight the role of SM as a receptor for EqtII.

SM is a derivative of sphingosine, with a fatty acid attached to the two-amino group through amide bonding. In mammals, this fatty acid usually has a long saturated acyl chain and, together with the sphingosine acyl chain, forms the hydrophobic part of the sphingolipids (19). Such a structure constitutes an excellent interaction partner for cholesterol, via both hydrogen bonding between the hydroxyl group of cholesterol and the amide group in the sphingosine, and hydrophobic interactions of the rigid cholesterol rings with the SM acyl chains (19). As a consequence of this differential interaction, L_o phases enriched in SM and cholesterol coexist with L_d phases in model membranes containing phosphatidylcholine, cholesterol, and SM over a large range of compositions, which include those mimicking the outer leaflet of the plasma membrane (24,26,31,34,44). Indeed, a similar situation is believed to occur in the plasma membrane of mammalian cells, where the preferential interaction of sphingolipids with cholesterol gives rise to small domains of transient nature known as lipid rafts (19). This notion is supported by experiments with dyes sensitive to

lipid environments that support the existence of L_o-like domains in the outer membrane of mammalian cells (45–47).

In our experiments with phase-segregated GUVs, EqtII bound preferentially to the L_o phase. This phase distribution is probably due to the enrichment of SM in the L_o phase, which acts as a specific receptor. But interestingly, a considerable amount of toxin concentrated at the phase boundaries. As shown by atomic force microscopy and crystallography studies, in model membranes the L_o phase is thicker than the L_d phase due to the higher conformational order of the acyl tails (33,48–52). To avoid the exposure of hydrophobic chains to the aqueous solvent, the lipids bend elastically at the domain interface, causing curvature stress, which has an energetic cost per length unit or line tension (26). As a consequence, there is a higher concentration of packing defects at the phase boundaries, which likely favor the binding of EqtII because of its amphipathic nature. A similar behavior has been observed for other proteins, including a peptide derived from helix 5 of Bax, PLA-2, and N-Ras (33,53,54). This may be a mechanism to increase the local concentration of EqtII and hence to reach the threshold for pore formation (40). Indeed, our experiments of membrane permeabilization in GUVs showed that at a certain toxin concentration, SM was not sufficient to promote pore opening, but phase coexistence was necessary. Interestingly, EqtII showed considerable permeabilizing activity in phase-separated GUVs without SM. The addition of a small amount of SM to phase-separated membranes, which would enhance EqtII binding, restored activity to almost 100% permeabilization.

Taken together, these observations highlight the dual role of SM in promoting EqtII activity. On one hand, it acts as a specific receptor for the toxin and promotes irreversible membrane binding (20,42). On the other hand, SM induces L_d-L_o phase separation in the presence of cholesterol (19), thus collaborating in the creation of lipid interfaces that increase the local concentration of EqtII and enhance pore opening. Interestingly, a comparable situation occurs in the case of the cholesterol-dependent cytolysins, an unrelated group of toxins that permeabilize membranes through the formation of β-barrel pores. Likewise, cholesterol is implied both in the binding process, acting as a receptor, and in the mechanism of pore formation (55). It is therefore tempting to hypothesize that SM- and cholesterol-dependent PFTs have evolved to use these features of the outer plasma membrane to optimize their activity. Concretely, they would do so by using lipids within lipid rafts as receptors and phase separation as a mechanism to increase local concentration. In fact, given the strong effect of phase separation on EqtII pore formation in model membranes, one may further speculate that its lytic activity in mammalian cells represents indirect evidence of phase separation in membranes.

This work was supported by a Marie Curie Intra-European Fellowship (to A.J.G.S.) within the 6th European Framework Program and Europäischen Fonds für regional Entwicklung (to E.F.R.E.) grant No. 4212/0608.

REFERENCES

1. Aroian, R., and F. G. van der Goot. 2007. Pore-forming toxins and cellular non-immune defenses (CNIDs). *Curr. Opin. Microbiol.* 10:57–61.
2. Tilley, S. J., and H. R. Saibil. 2006. The mechanism of pore formation by bacterial toxins. *Curr. Opin. Struct. Biol.* 16:230–236.
3. Kristan, K., Z. Podlesek, V. Hojnik, I. Gutierrez-Aguirre, G. Guncar, D. Turk, J. M. Gonzalez-Manas, J. H. Lakey, P. Macek, and G. Anderluh. 2004. Pore formation by equinatoxin, a eukaryotic pore-forming toxin, requires a flexible N-terminal region and a stable beta-sandwich. *J. Biol. Chem.* 279:46509–46517.
4. Olson, R., and E. Gouaux. 2005. Crystal structure of the Vibrio cholerae cytolysin (VCC) pro-toxin and its assembly into a heptameric transmembrane pore. *J. Mol. Biol.* 350:997–1016.
5. Heuck, A. P., R. K. Tweten, and A. E. Johnson. 2001. Beta-barrel pore-forming toxins: intriguing dimorphic proteins. *Biochemistry.* 40:9065–9073.
6. Yang, L., T. A. Harroun, T. M. Weiss, L. Ding, and H. W. Huang. 2001. Barrel-stave model or toroidal model? A case study on melittin pores. *Biophys. J.* 81:1475–1485.
7. Leontiadou, H., A. E. Mark, and S. J. Marrink. 2006. Antimicrobial peptides in action. *J. Am. Chem. Soc.* 128:12156–12161.
8. Anderluh, G., and P. Macek. 2002. Cytolytic peptide and protein toxins from sea anemones (*Anthozoa: actiniaria*). *Toxicon.* 40:111–124.
9. Athanasiadis, A., G. Anderluh, P. Macek, and D. Turk. 2001. Crystal structure of the soluble form of Equinatoxin II, a pore-forming toxin from the sea anemone Actinia equina. *Structure.* 9:341–346.
10. Hinds, M. G., W. Zhang, G. Anderluh, P. E. Hansen, and R. S. Norton. 2002. Solution structure of the eukaryotic pore-forming cytolysin Equinatoxin II: implications for pore formation. *J. Mol. Biol.* 315: 1219–1229.
11. Malovrh, P., G. Viero, M. D. Serra, Z. Podlesek, J. H. Lakey, P. Macek, G. Menestrina, and G. Anderluh. 2003. A novel mechanism of pore formation: membrane penetration by the N-terminal amphipathic region of equinatoxin. *J. Biol. Chem.* 278:22678–22685.
12. Hong, Q., I. Gutierrez-Aguirre, A. Barlic, P. Malovrh, K. Kristan, Z. Podlesek, P. Macek, D. Turk, J. M. Gonzalez-Manas, J. H. Lakey, and G. Anderluh. 2002. Two-step membrane binding by Equinatoxin II, a pore-forming toxin from the sea anemone, involves an exposed aromatic cluster and a flexible helix. *J. Biol. Chem.* 277:41916–41924.
13. Anderluh, G., A. Barlic, Z. Podlesek, P. Macek, J. Pungercar, F. Gubensek, M. L. Zecchini, M. D. Serra, and G. Menestrina. 1999. Cysteine-scanning mutagenesis of an eukaryotic pore-forming toxin from sea anemone: topology in lipid membranes. *Eur. J. Biochem.* 263:128–136.
14. Malovrh, P., A. Barlic, Z. Podlesek, P. Macek, G. Menestrina, and G. Anderluh. 2000. Structure-function studies of tryptophan mutants of Equinatoxin II, a sea anemone pore-forming protein. *Biochem. J.* 346:223–232.
15. Kristan, K., G. Viero, P. Macek, S. M. Dalla, and G. Anderluh. 2007. The equinatoxin N-terminus is transferred across planar lipid membranes and helps to stabilize the transmembrane pore. *FEBS J.* 274: 539–550.
16. Anderluh, G., S. M. Dalla, G. Viero, G. Guella, P. Macek, and G. Menestrina. 2003. Pore formation by Equinatoxin II, a eukaryotic protein toxin, occurs by induction of nonlamellar lipid structures. *J. Biol. Chem.* 278:45216–45223.
17. Belmonte, G., C. Pederzolli, P. Macek, and G. Menestrina. 1993. Pore formation by the sea anemone cytolysin Equinatoxin II in red blood cells and model lipid membranes. *J. Membr. Biol.* 131:11–22.
18. Anderluh, G., A. Razpotnik, Z. Podlesek, P. Macek, F. Separovic, and R. S. Norton. 2005. Interaction of the eukaryotic pore-forming cytolysin Equinatoxin II with model membranes: 19F NMR studies. *J. Mol. Biol.* 347:27–39.
19. Simons, K., and W. L. Vaz. 2004. Model systems, lipid rafts, and cell membranes. *Annu. Rev. Biophys. Biomol. Struct.* 33:269–295.

20. Barlic, A., I. Gutierrez-Aguirre, J. M. Caaveiro, A. Cruz, M. B. Ruiz-Arguello, J. Perez-Gil, and J. M. Gonzalez-Manas. 2004. Lipid phase coexistence favors membrane insertion of Equinatoxin-II, a pore-forming toxin from Actinia equina. *J. Biol. Chem.* 279:34209–34216.

21. Ambroggio, E. E., D. H. Kim, F. Separovic, C. J. Barrow, K. J. Barnham, L. A. Bagatolli, and G. D. Fidelio. 2005. Surface behavior and lipid interaction of Alzheimer β-amyloid peptide 1–42: a membrane-disrupting peptide. *Biophys. J.* 88:2706–2713.

22. Farge, E., and P. F. Devaux. 1992. Shape changes of giant liposomes induced by an asymmetric transmembrane distribution of phospholipids. *Biophys. J.* 61:347–357.

23. Bacia, K., P. Schwille, and T. Kurzchalia. 2005. Sterol structure determines the separation of phases and the curvature of the liquid-ordered phase in model membranes. *Proc. Natl. Acad. Sci. USA.* 102:3272–3277.

24. Baumgart, T., S. T. Hess, and W. W. Webb. 2003. Imaging coexisting fluid domains in biomembrane models coupling curvature and line tension. *Nature.* 425:821–824.

25. Kahya, N., D. Scherfeld, K. Bacia, B. Poolman, and P. Schwille. 2003. Probing lipid mobility of raft-exhibiting model membranes by fluorescence correlation spectroscopy. *J. Biol. Chem.* 278:28109–28115.

26. Garcia-Saez, A. J., S. Chiantia, and P. Schwille. 2007. Effect of line tension on the lateral organization of lipid membranes. *J. Biol. Chem.* 282:33537–33544.

27. Ambroggio, E. E., F. Separovic, J. H. Bowie, G. D. Fidelio, and L. A. Bagatolli. 2005. Direct visualization of membrane leakage induced by the antibiotic peptides: maculatin, citropin, and aurein. *Biophys. J.* 89: 1874–1881.

28. Tamba, Y., and M. Yamazaki. 2005. Single giant unilamellar vesicle method reveals effect of antimicrobial peptide magainin 2 on membrane permeability. *Biochemistry.* 44:15823–15833.

29. Mally, M., J. Majhenc, S. Svetina, and B. Zeks. 2002. Mechanisms of Equinatoxin II-induced transport through the membrane of a giant phospholipid vesicle. *Biophys. J.* 83:944–953.

30. Dimitrov, D. S., and M. I. Angelova. 1988. Lipid swelling and liposome formation mediated by electric-fields. *Bioelectrochem. Bioenerg.* 19:323–336.

31. Bacia, K., D. Scherfeld, N. Kahya, and P. Schwille. 2004. Fluorescence correlation spectroscopy relates rafts in model and native membranes. *Biophys. J.* 87:1034–1043.

32. Reference deleted in proof.

33. Garcia-Saez, A. J., S. Chiantia, J. Salgado, and P. Schwille. 2007. Pore formation by a Bax-derived peptide: effect on the line tension of the membrane probed by AFM. *Biophys. J.* 93:103–112.

34. Chiantia, S., J. Ries, N. Kahya, and P. Schwille. 2006. Combined AFM and two-focus SFCS study of raft-exhibiting model membranes. *ChemPhysChem.* 7:2409–2418.

35. Valcarcel, C. A., S. M. Dalla, C. Potrich, I. Bernhart, M. Tejuca, D. Martinez, F. Pazos, M. E. Lanio, and G. Menestrina. 2001. Effects of lipid composition on membrane permeabilization by sticholysin I and II, two cytolysins of the sea anemone Stichodactyla helianthus. *Biophys. J.* 80:2761–2774.

36. Schwartz, J. L., L. Potvin, F. Coux, J. F. Charles, C. Berry, M. J. Humphreys, A. F. Jones, I. Bernhart, S. M. Dalla, and G. Menestrina. 2001. Permeabilization of model lipid membranes by Bacillus sphaericus mosquitocidal binary toxin and its individual components. *J. Membr. Biol.* 184:171–183.

37. Dalla, S. M., and G. Menestrina. 2003. Liposomes in the study of pore-forming toxins. *Methods Enzymol.* 372:99–124.

38. Garcia-Saez, A. J., M. Coraiola, S. M. Dalla, I. Mingarro, G. Menestrina, and J. Salgado. 2005. Peptides derived from apoptotic Bax and Bid reproduce the poration activity of the parent full-length proteins. *Biophys. J.* 88:3976–3990.

39. Tamba, Y., S. Ohba, M. Kubota, H. Yoshioka, H. Yoshioka, and M. Yamazaki. 2007. Single GUV method reveals interaction of tea catechin (−)-epigallocatechin gallate with lipid membranes. *Biophys. J.* 92:3178–3194.

40. Huang, H. W., F. Y. Chen, and M. T. Lee. 2004. Molecular mechanism of peptide-induced pores in membranes. *Phys. Rev. Lett.* 92:198304.

41. Karatekin, E., O. Sandre, H. Guitouni, N. Borghi, P. H. Puech, and F. Brochard-Wyart. 2003. Cascades of transient pores in giant vesicles: line tension and transport. *Biophys. J.* 84:1734–1749.

42. Caaveiro, J. M., I. Echabe, I. Gutierrez-Aguirre, J. L. Nieva, J. L. Arrondo, and J. M. Gonzalez-Manas. 2001. Differential interaction of Equinatoxin II with model membranes in response to lipid composition. *Biophys. J.* 80:1343–1353.

43. Reference deleted in proof.

44. Veatch, S. L., and S. L. Keller. 2005. Miscibility phase diagrams of giant vesicles containing sphingomyelin. *Phys. Rev. Lett.* 94:148101.

45. Gaus, K., E. Gratton, E. P. W. Kable, A. S. Jones, I. Gelissen, L. Kritharides, and W. Jessup. 2003. Visualizing lipid structure and raft domains in living cells with two-photon microscopy. *Proc. Natl. Acad. Sci. USA.* 100:15554–15559.

46. Gidwani, A., D. Holowka, and B. Baird. 2001. Fluorescence anisotropy measurements of lipid order in plasma membranes and lipid rafts from RBL-2H3 mast cells. *Biochemistry.* 40:12422–12429.

47. Ge, M., A. Gidwani, H. A. Brown, D. Holowka, B. Baird, and J. H. Freed. 2003. Ordered and disordered phases coexist in plasma membrane vesicles of RBL-2H3 mast cells. An ESR study. *Biophys. J.* 85: 1278–1288.

48. Chiantia, S., N. Kahya, and P. Schwille. 2005. Dehydration damage of domain-exhibiting supported bilayers: an AFM study on the protective effects of disaccharides and other stabilizing substances. *Langmuir.* 21:6317–6323.

49. Kuzmin, P. I., S. A. Akimov, Y. A. Chizmadzhev, J. Zimmerberg, and F. S. Cohen. 2005. Line tension and interaction energies of membrane rafts calculated from lipid splay and tilt. *Biophys. J.* 88:1120–1133.

50. Rinia, H. A., M. M. Snel, J. P. van der Eerden, and B. de Kruijff. 2001. Visualizing detergent resistant domains in model membranes with atomic force microscopy. *FEBS Lett.* 501:92–96.

51. Garcia-Saez, A. J., and P. Schwille. 2007. Single molecule techniques for the study of membrane proteins. *Appl. Microbiol. Biotechnol.* 76: 257–266.

52. Gandhavadi, M., D. Allende, A. Vidal, S. A. Simon, and T. J. McIntosh. 2002. Structure, composition, and peptide binding properties of detergent soluble bilayers and detergent resistant rafts. *Biophys. J.* 82:1469–1482.

53. Nicolini, C., J. Baranski, S. Schlummer, J. Palomo, M. Lumbierres-Burgues, M. Kahms, J. Kuhlmann, S. Sanchez, E. Gratton, H. Waldmann, and R. Winter. 2006. Visualizing association of N-Ras in lipid microdomains: influence of domain structure and interfacial adsorption. *J. Am. Chem. Soc.* 128:192–201.

54. Staneva, G., M. I. Angelova, and K. Koumanov. 2004. Phospholipase A2 promotes raft budding and fission from giant liposomes. *Chem. Phys. Lipids.* 129:53–62.

55. Giddings, K. S., A. E. Johnson, and R. K. Tweten. 2003. Redefining cholesterol's role in the mechanism of the cholesterol-dependent cytolysins. *Proc. Natl. Acad. Sci. USA.* 100:11315–11320.